

The Autler-Townes effect revisited

Claude Cohen-Tannoudji

*Collège de France et Laboratoire Kastler Brossel
de l'Ecole Normale Supérieure*
24 rue Lhomond, 75231 Paris Cedex 05, France*

In 1955, Autler and Townes showed that a microwave transition of the OCS molecule can split into two components when one of the two levels involved in the transition is coupled to a third one by a strong resonant microwave field [1]. The corresponding doublet is called the Autler-Townes doublet, or the dynamic Stark splitting. Such an effect is in fact quite general. Using a dressed-atom approach, I would like to show in this paper that the basic features of the Autler-Townes effect show themselves in several new research fields, such as high resolution optical spectroscopy, cavity quantum electrodynamics and laser cooling. This will be a way for me to express my admiration and gratitude to Charles Townes. My admiration for the fundamental concepts that he has so fruitfully introduced in so many different branches of physics ; my gratitude for all that I have learned from his writings and his lectures.

1 Dressed-atom approach to the Autler-Townes effect

The first theoretical treatment of the Autler-Townes effect used a semi-classical theory where the strong resonant microwave field is described as a c -number sinusoidal field. Such a description is perfectly valid and can be rigorously justified when the driving field is in a coherent state [2]. Quantizing the driving field, however, provides interesting physical insights. Although not essential, such a quantum treatment dealing with the total coupled system “atom + driving photons”, also called “dressed atom”, has the advantage of correlating all the observable phenomena with the properties of the energy diagram of a time-independent Hamiltonian. In particular, the Autler-Townes effect is associated with a level anticrossing in this energy diagram [3]. Furthermore, in certain new domains, like cavity quantum electrodynamics, the quantization of the field becomes essential. We will therefore introduce here the Autler-Townes effect from a dressed-atom point of view. We will restrict ourselves to the essential points which will be useful for the discussions presented in the next sections. More details about the dressed-atom approach may be found elsewhere [4].

We consider a three-level atom a , b , c (Fig. 1), with two allowed transitions $a \longleftrightarrow b$ and $b \longleftrightarrow c$, the energy splittings being $\hbar\omega_0$ and $\hbar\omega'_0$, respectively. An intense quasi-resonant field, with frequency ω_L , drives the transition $a \longleftrightarrow b$. The detuning

$$\delta = \omega_L - \omega_0 \tag{1}$$

between ω_L and ω_0 is very small compared to ω_0 and ω'_0 . The difference between ω_0 and ω'_0 is sufficiently large to allow one to consider the field ω_L as being completely nonresonant for the transition $b \longleftrightarrow c$. A very weak field with frequency ω probes the transition $b \longleftrightarrow c$. The problem is to understand how the absorption of the probe field is modified when the transition $a \longleftrightarrow b$ is driven by the field ω_L .

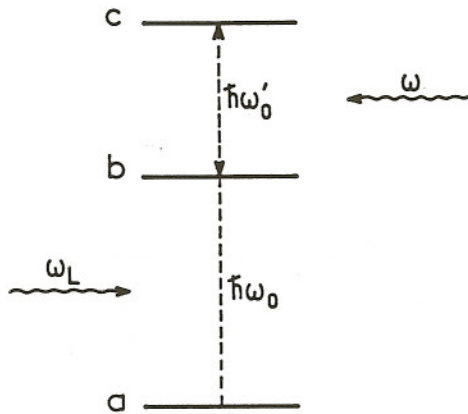


Figure 1: Three-level atom. The intense quasi-resonant field ω_L drives the transition $a \longleftrightarrow b$. The weak field ω probes the transition $b \longleftrightarrow c$.

The Hamiltonian H of the atom dressed by the field ω_L may be written

$$H = H_A + H_L + V_{AL} \quad (2)$$

where H_A is the atomic Hamiltonian, H_L the Hamiltonian of the field mode L corresponding to the driving field, and V_{AL} the atom-field coupling. The left part of Fig. 2 represents a few eigenstates of $H_A + H_L$ (uncoupled states), labelled by two quantum numbers, one (a , b or c) for the atom, and one (N) for the number of photons ω_L . The two states $|a, N+1\rangle$ (atom in a in the presence of $N+1$ photons ω_L) and $|b, N\rangle$ (atom in b in the presence of N photons) are separated by a distance $E_a + (N+1)\hbar\omega_L - E_b - N\hbar\omega_L = \hbar(\omega_L - \omega_0) = \hbar\delta$ which is very small compared to the distance $\hbar\omega'_0$ between $|c, N\rangle$ and $|b, N\rangle$. At resonance ($\delta = 0$), the two states $|a, N+1\rangle$ and $|b, N\rangle$ are degenerate. The interaction Hamiltonian V_{AL} couples these two states: the atom in the state $|a\rangle$ can absorb one photon ω_L and go to the state $|b\rangle$.

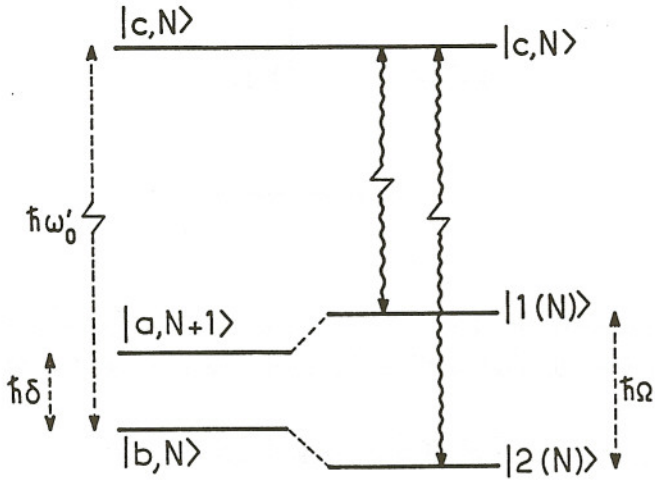


Figure 2: A few uncoupled states (left part) and corresponding perturbed or dressed states (right part) of the atom + photons ω_L system. The dotted lines indicate the energy splittings between states. The wavy lines give the allowed transitions between dressed states which can be probed by the weak field ω .

The corresponding matrix element is written

$$\langle b, N | V_{AL} | a, N + 1 \rangle = \hbar\Omega_1/2 \quad (3)$$

where Ω_1 is the so-called ‘‘Rabi frequency’’ which is proportional to the field amplitude and to the transition dipole moment between a and b . Strictly speaking, Ω_1 is proportional to $\sqrt{N+1}$ and thus depends on N . We shall neglect this dependence here, assuming that the field ω_L is initially excited in a coherent state with a Poisson distribution for N having a width ΔN much smaller than the mean value $\langle N \rangle$ of N . As a result of the coupling (3), the two uncoupled states $|a, N + 1\rangle$ and $|b, N\rangle$ repel each other and are transformed into two perturbed or dressed states $|1(N)\rangle$ and $|2(N)\rangle$, which are given by two orthogonal linear combinations of $|a, N + 1\rangle$ and $|b, N\rangle$ whose energies are separated by a distance $\hbar\Omega$ with

$$\Omega = \sqrt{\Omega_1^2 + \delta^2} \quad (4)$$

(see right part of Fig. 2). Because we assume that the field ω_L is completely off resonance for the transition $b \longleftrightarrow c$, we neglect any effect of V_{AL} on $|c, N\rangle$.

The transitions with frequencies close to ω'_0 which are probed by the weak field ω are those which reduce to the transition $|c, N\rangle \longleftrightarrow |b, N\rangle$ in the limit $\Omega_1 \longrightarrow 0$. Because the two dressed states $|1(N)\rangle$ and $|2(N)\rangle$ contain both admixtures of $|b, N\rangle$, we see that the two transitions $|c, N\rangle \longleftrightarrow |1(N)\rangle$ and $|c, N\rangle \longleftrightarrow |2(N)\rangle$, represented by the wavy lines of Fig. 2, are both allowed for the probe field. The absorption spectrum of this probe field, which reduces to a single line of frequency ω'_0 in the absence of V_{AL} becomes a doublet when the $a \longleftrightarrow b$ transition is driven by the field ω_L . This is the Autler-Townes doublet.

In order to understand how the frequencies of the two lines of the doublet vary with the detuning δ of the driving field, it is convenient to introduce an energy diagram giving the energies of the dressed states of Fig. 2 versus $\hbar\omega_L$ (see Fig. 3). The uncoupled state $|a, N\rangle$ is chosen as the energy origin.

The energies of the uncoupled states $|b, N\rangle$ and $|c, N\rangle$ are then represented by horizontal dashed lines with ordinates equal to $\hbar\omega_0$ and $\hbar(\omega_0 + \omega'_0)$, respectively. The energy of $|a, N + 1\rangle$ is represented by a dashed straight line with slope 1 passing through the origin and intersecting the horizontal line associated with $|b, N\rangle$ at $\hbar\omega_L = \hbar\omega_0$. When the effect of V_{AL} is taken into account, we get the two dressed states $|1(N)\rangle$ and $|2(N)\rangle$, represented by the solid lines of Fig. 3, which form the two branches of a hyperbola having the above-mentioned dashed lines as asymptotes. The minimum distance between the two branches of the hyperbola occurs for $\hbar\omega_L = \hbar\omega_0$ and is equal to $\hbar\Omega_1$. Finally, the state $|c, N\rangle$ is (in the neighbourhood of $\hbar\omega_L = \hbar\omega_0$) unaffected by the coupling V_{AL} and remains represented by a horizontal line.

The effect of the coupling V_{AL} is thus to transform the crossing between $|a, N + 1\rangle$ and $|b, N\rangle$, which occurs at $\hbar\omega_L = \hbar\omega_0$, into an “anticrossing”. One clearly sees in Fig. 3 how the two components of the Autler-Townes doublet, represented by the wavy arrows, vary with the detuning. At resonance ($\omega_L = \omega_0$), one gets two lines with frequencies $\omega'_0 \pm (\Omega_1/2)$. Off resonance ($|\delta| \gg \Omega_1$), one of the two lines of the doublet has a frequency close to ω'_0 , the other line a frequency close to $\omega_0 + \omega'_0 - \omega_L$. By evaluating the admixture of $|b, N\rangle$ in each dressed state, one can determine the intensities of the two components of the doublet. One finds that they are equal at resonance, whereas the line with a frequency close to ω'_0 becomes the most intense off-resonance. Note that, near the asymptotes of Fig. 3, i.e. for $|\delta| \gg \Omega_1$, the distance between each dressed state and its corresponding asymptote is nothing but the ac Stark shift of level a or b due to its coupling with the field ω_L which is then nonresonant. If ω_L lies in the optical domain, such a shift is also called light shift and it has been observed in optical pumping experiments [5].

In the previous discussion, we have neglected the width γ of the levels due to various damping processes such as spontaneous emission and collisions. We have supposed implicitly that the Rabi frequency Ω_1 is sufficiently large compared to γ . Such a situation corresponds to a “strong coupling” regime where the two lines of the doublet are clearly resolved, even at resonance.

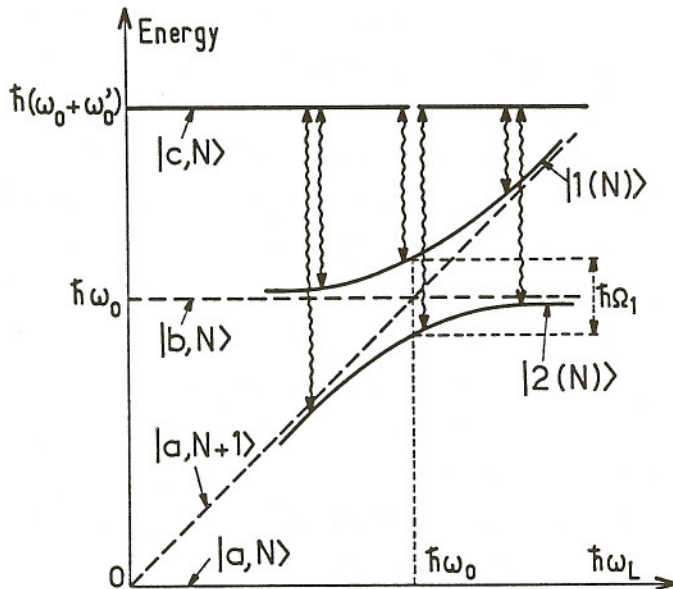


Figure 3: Energies of the dressed states of Fig. 2 (solid lines) versus $\hbar\omega_L$. The dashed lines represent the energies of the uncoupled states. Whereas the two uncoupled states $|a, N + 1\rangle$ and $|b, N\rangle$ cross for $\hbar\omega_L = \hbar\omega_0$, the two dressed states $|1(N)\rangle$ and $|2(N)\rangle$ form an “anticrossing”. The wavy lines represent, for different values of $\hbar\omega_L$, the two components of the Autler-Townes doublet.

2 The Autler-Townes effect in the optical domain

The spectacular development of laser sources in the early seventies stimulated several experimental and theoretical studies dealing with the behaviour of atoms submitted to intense monochromatic optical fields. The light intensity became high enough to achieve Rabi frequencies larger than the width of the levels. The tunability of laser sources allowed also the frequency of the laser light to be continuously varied across the atomic frequency. Finally, spontaneous emission of radiation, which is negligible in the microwave and RF domains, becomes important in the optical domain and gives rise to new types of signals, such as the intensity or the spectral distribution of the fluorescence light, which can be used for probing the consequences of the laser-atom interaction. Note also that the Doppler effect is important for optical lines and must be taken into account for moving atoms. We briefly review in this section a few experiments showing how the Autler-Townes effect manifests itself in the optical domain.

2.1 Case of two optical transitions sharing a common level

Such a case corresponds to a straightforward extension of the experiments performed in the microwave domain. One intense laser field ω_L drives an optical transition $a \longleftrightarrow b$. A second weak laser field probes a second transition $b \longleftrightarrow c$ sharing a common level b with the first transition. The three levels a, b, c can form a “cascade” configuration as in Fig. 1, or a V -configuration, or a Λ -configuration.

A few experiments used an atomic beam, perpendicular to both the driving and probe laser fields [6], in which case the Doppler effect for both transitions vanishes. The detection signal is then the intensity I_F of the fluorescence light emitted from level c (or from excited levels populated from c),

which is proportional to the population of level c , and also to the absorption of the probe field ω . A clear splitting of the curve giving I_F versus ω , for a fixed resonant value of ω_L , was observed, giving evidence for an Autler-Townes splitting of the optical line $b \longleftrightarrow c$. It was also checked that the frequency splitting between the two components of the doublet was proportional to $\sqrt{I_L}$, where I_L is the intensity of the driving field ω_L , as expected for a Rabi frequency which is proportional to the laser electric field.

A few experiments have been also performed with atomic vapors [7]. The Doppler width of optical lines is generally much larger than the natural width of the atomic states. As a consequence of the large Doppler shifts which modify ω_L and ω for a moving atom, the Autler-Townes splitting of the $b \longleftrightarrow c$ line generally washes out when the average is taken over atomic velocities. It may be shown, however, that narrow Doppler-free structures can survive in certain conditions the Doppler averaging and give evidence for the Autler-Townes splitting of the $b \longleftrightarrow c$ line [8]. For example, for the cascade configuration of Fig. 1, the driving field ω_L and the probe field must propagate in opposite directions. Simple graphic constructions, using energy diagrams analogous to the one of Fig. 3, have been proposed for interpreting these narrow Doppler-free structures [9]. They lead to the idea that the Doppler effect can be compensated by velocity-dependent light shifts [10]. Experiments have been performed to demonstrate this idea [11].

2.2 Single optical transition - The Mollow triplet

Suppose now that the probe field ω is switched off and that we have a single laser beam with frequency ω_L driving the $a \longleftrightarrow b$ transition. For detecting the perturbation of the $a \longleftrightarrow b$ transition by the field ω_L , we use the fluorescence light spontaneously emitted by the atom from the excited state b . More precisely, we consider the spectral distribution of this fluorescence light. Using optical Bloch equations, Mollow [12] has calculated the correlation function of the atomic dipole moment and shown that, at high intensity

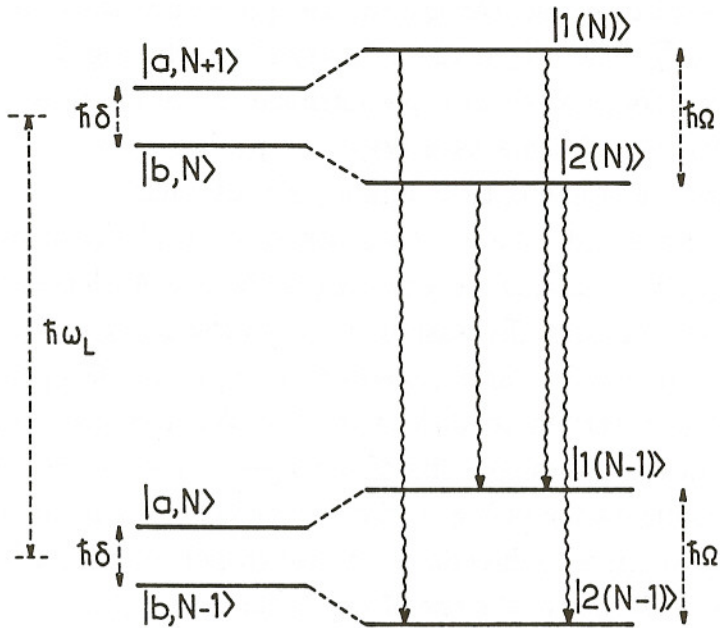


Figure 4: Dressed atom interpretation of the Mollow fluorescence triplet. The left part of the figure represents two adjacent manifolds of uncoupled states, the right part the corresponding Autler-Townes doublets of dressed states. The wavy arrows give the allowed transitions between dressed states whose frequencies give the centers of the various components of the fluorescence spectrum.

or large detuning ($|\delta|$ or $\Omega_1 \gg$ natural width Γ), the fluorescence spectrum consists of a triplet. Several groups have observed experimentally such a triplet [13].

We will not discuss here the various features of the Mollow fluorescence triplet. We just want to point out that it can be related, as the Autler-Townes effect, to the existence of doublets of dressed states [14]. The left part of Fig. 4 represents two adjacent manifolds of uncoupled states, analogous to the one of Fig. 2: $\{|a, N+1\rangle, |b, N\rangle\}$ and $\{|a, N\rangle, |b, N-1\rangle\}$. Since $|a, N+1\rangle$ and $|a, N\rangle$ differ by one laser photon, as well as $|b, N\rangle$ and $|b, N-1\rangle$, the distance between the two manifolds is $\hbar\omega_L$. When the coupling V_{AL} is taken into account, one gets the two doublets of dressed states $\{|1(N)\rangle, |2(N)\rangle\}$ and $\{|1(N-1)\rangle, |2(N-1)\rangle\}$ represented in the right part of Fig. 4. In each doublet the splitting is $\hbar\Omega$, and the distance between the two doublets is $\hbar\omega_L$. The allowed spontaneous transitions between dressed states correspond to pairs of levels between which the atomic dipole moment operator \mathbf{d} has a nonzero matrix element. In the uncoupled basis, \mathbf{d} , which cannot change the quantum number N , couples only $|b, N\rangle$ and $|a, N\rangle$. The two dressed states $|1(N)\rangle$ and $|2(N)\rangle$ are both “contaminated” by $|b, N\rangle$. Similarly, the two dressed states $|1(N-1)\rangle$ and $|2(N-1)\rangle$ are both contaminated by $|a, N\rangle$. It follows that the four transitions connecting $|1(N)\rangle$ and $|2(N)\rangle$ to $|1(N-1)\rangle$ and $|2(N-1)\rangle$ are allowed (wavy lines of Fig. 4). One immediately understands in this way why the fluorescence spectrum consists of three lines with frequencies $\omega_L + \Omega$, $\omega_L - \Omega$ and ω_L associated with the transitions $|1(N)\rangle \rightarrow |2(N-1)\rangle$, $|2(N)\rangle \rightarrow |1(N-1)\rangle$ and $|i(N)\rangle \rightarrow |i(N-1)\rangle$ (with $i = 1, 2$), respectively. We suppose here that Ω is large compared to the natural width Γ , so that the three lines are well resolved. According to (4), such a condition is equivalent to $\Omega_1 \gg \Gamma$ or $|\delta| \gg \Gamma$.

3 The Autler-Townes effect in cavity quantum electrodynamics

In the previous discussion, the number N of photons is not a well-defined quantity. The field is quantized in a fictitious box, having a volume V which can be arbitrarily large. Only the energy density N/V at the position of the atom is relevant to the experiment being analyzed.

During the last few years, spectacular progress has been made allowing one to study the behavior of atoms put in resonant cavities having a very high finesse. In such (real) cavities, the number N of photons has a definite meaning. For example, the cavity can be empty ($N = 0$) and one can then study how the spontaneous emission rates and the Lamb shift are modified by the boundary conditions imposed by the cavity walls. By introducing excited atoms in the cavity, one can produce a maser or a laser action with a very small number of atoms and a very small number of photons. For a survey of the field, we refer the reader to recent reviews [15]. We will focus here on an effect usually called “vacuum Rabi splitting” in cavity quantum electrodynamics and which is in fact quite similar to the Autler-Townes effect. We will use the so-called Jaynes-Cummings model [16]. This model is quite similar to the dressed-atom model used in the previous sections, except that the two-level atom is now coupled to a single mode of an actual cavity, so that N can take very small values and it is no longer possible to neglect the variations with N of the Rabi frequency.

The left part of Fig. 5 represents a few uncoupled states of the system formed by a two-level atom $a - b$ with frequency ω_0 and a single mode field of the cavity with frequency ω_L . The state $|a, 0\rangle$ (atom in the lower state a with 0 photon in the cavity) is nondegenerate and has the lowest energy. We suppose that the cavity is resonant ($\omega_L = \omega_0$), so that the two states $|a, 1\rangle$ and $|b, 0\rangle$ are degenerate, as well as $|a, 2\rangle$ and $|b, 1\rangle$. When the atom-field coupling V_{AL} is taken into account, one finds that level $|a, 0\rangle$ is not perturbed (in the rotating wave approximation). Levels $|a, 1\rangle$ and $|b, 0\rangle$ are coupled by V_{AL} , as

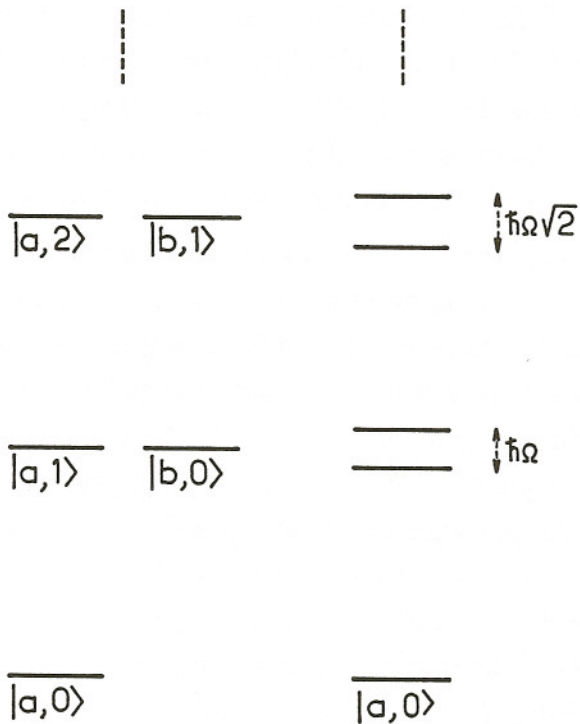


Figure 5: Uncoupled states (left part) and coupled or dressed states (right part) of the atom-cavity mode system.

well as $|a, 2\rangle$ and $|b, 1\rangle$. One thus gets the series of doublets of dressed states represented in the right part of Fig. 5. Since $\langle a, N | V_{AL} | b, N-1 \rangle$ varies as \sqrt{N} , the splittings of the first two doublets are equal to $\hbar\Omega$ and $\hbar\Omega\sqrt{2}$, respectively. The frequency Ω can be considered as the Rabi frequency corresponding to the field associated with a single photon in the cavity. We suppose here that we are in a strong coupling regime : the damping rate of the field in the cavity and the damping rate of the atom are slow enough compared to Ω that the two dressed states of each doublet are well resolved.

Suppose now that a very weak probe field with frequency ω close to ω_L is sent through the cavity and that one measures the transmission $T(\omega)$ of the cavity versus ω . Initially, no photon is present in the cavity which contains a single atom in the lower state a , so that the total system is in the state $|a, 0\rangle$. The probe field can enter into the cavity only if its frequency ω coincides with an eigenfrequency of the cavity. The frequencies of the new modes of the cavity in the presence of the atom-field coupling are the frequencies of the two transitions connecting $|a, 0\rangle$ to the first two dressed states of Fig. 5. One thus expects the transmission spectrum $T(\omega)$ to exhibit two peaks at $\omega = \omega_L \pm (\Omega/2)$. In particular, if the two peaks are well resolved, $T(\omega)$ can become negligible in the middle, i.e. when $\omega = \omega_L$. This means that a resonant probe field $\omega = \omega_L$ which can enter into the empty cavity is reflected from the cavity if the cavity contains a single atom. All the previous results can be easily extended to the case where the cavity contains n identical atoms instead of 1. If the coupling is symmetric, i.e. if all atoms are identically coupled to the field, one can show that the first doublet above the ground state has a splitting $\hbar\Omega\sqrt{n}$ instead of $\hbar\Omega$.

Recent experiments [17] have reached the strong coupling regime and have allowed the observation of a doublet in the transmission spectrum of a probe field in conditions where the cavity contains a very small number of atoms, down to 1. This shows that the physical mechanism responsible for the Autler-Townes effect (transitions involving doublets of dressed states) can give rise to observable phenomena even in the limit of a single atom

coupled to a single photon.

4 Doublets of dressed states with a position dependent Rabi frequency

We come back to an atom in free space, which we suppose to interact with a laser electric field varying in space. The Rabi frequency $\Omega_1(\mathbf{r})$ characterizing the atom-field coupling for an atom at \mathbf{r} thus depends on \mathbf{r} . By considering, as in the previous sections, doublets of dressed states, which now have position-dependent splittings and position-dependent widths, we want to show in this section that it is possible to get physical insights into important features of the radiative forces which govern atomic motion in laser light. This will be another example of the close connections which exist between the Autler-Townes effect and new research fields, such as laser cooling and trapping.

4.1 Gradient (or dipole) forces

The splitting $\hbar\Omega$ between the two dressed states $|1(N)\rangle$ and $|2(N)\rangle$ of Fig. 2 increases when the Rabi frequency Ω_1 increases [see equation (4)]. Figure 6 gives the variations of the energies of these two dressed states when the position of the atom is varied across a laser beam with a finite waist. Inside the laser beam, Ω_1 is large and the splitting between the dressed states is large. Outside the laser beam, this splitting tends to a constant value $\hbar\delta$, equal to the energy separation between the uncoupled states $|a, N+1\rangle$ and $|b, N\rangle$, and the dressed states tend to the uncoupled states. For a positive detuning ($\omega_L > \omega_0$), $|a, N+1\rangle$ is above $|b, N\rangle$, so that $|1(N)\rangle$ and $|2(N)\rangle$ tend to $|a, N+1\rangle$ and $|b, N\rangle$, respectively, outside the laser beam (Fig. 6 α). For $\omega_L < \omega_0$, the previous conclusions are reversed (Fig. 6 β).

Consider now an atom, initially at rest, at a certain position in the laser beam and suppose that it is in a certain dressed state. Because the dressed state energy is position-dependent, the atom experiences a gradient

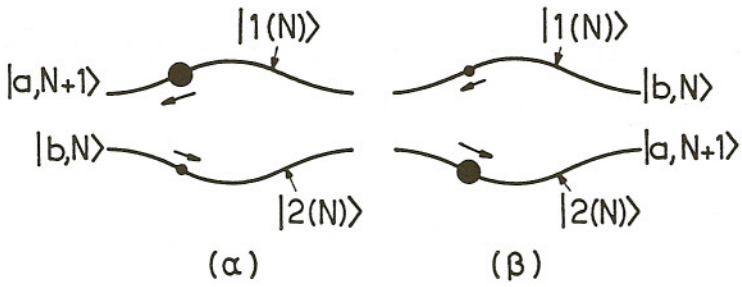


Figure 6: Energies of the two dressed states $|1(N)\rangle$ and $|2(N)\rangle$ versus the position of the atom across a laser beam. The splitting between the dressed states is maximum in the center of the laser beam. Outside the laser beam the dressed states tend to the uncoupled states $|a, N+1\rangle$ and $|b, 1\rangle$. Figures 6 α and 6 β correspond to $\delta > 0$ ($\omega_L > \omega_0$) and $\delta < 0$ ($\omega_L < \omega_0$), respectively. The size of each filled circle is proportional to the probability of occupation of the corresponding dressed state.

force whose direction is indicated by the arrows of Fig. 6. If the atom is in the other dressed state, the gradient force has the opposite sign. To get the mean gradient force experienced by the atom, one must average the gradient forces associated with each dressed state using the probability of occupation Π_1 or Π_2 of these states which are indicated by the size of the filled circles of Fig. 6. For $\delta > 0$ (Fig. 6 α), the dressed state $|2(N)\rangle$, which tends to $|b, N\rangle$ outside the laser beam, is more contaminated by the unstable state $|b, N\rangle$ than $|1(N)\rangle$ is. It is therefore less populated than $|1(N)\rangle$, because it has a shorter lifetime : $\Pi_1 > \Pi_2$. The sign of the mean gradient force is thus determined by the sign of the gradient force associated with $|1(N)\rangle$ and this explains why the atom is expelled from the high intensity regions when $\omega_L > \omega_0$. For $\omega_L < \omega_0$ (Fig. 6 β) these conclusions are reversed and the atom is attracted towards the high intensity regions. This explains how an atom can be trapped in a focal zone of a red detuned laser beam. For $\omega_L = \omega_0$,

the two dressed states contain equal admixtures of $|b, N\rangle$, they are equally populated, and the mean gradient force vanishes.

The previous picture gives also a simple interpretation of the fluctuations of gradient forces. Consider the radiative transitions induced by spontaneous emission between doublets of dressed states (see the wavy lines of Fig. 4). They are at the origin of a radiative cascade of the dressed atom falling down its ladder of dressed states. For example, the dressed atom can jump from $|1(N)\rangle$ to $|2(N-1)\rangle$, then from $|2(N-1)\rangle$ to $|1(N-2)\rangle$ and so on. The probabilities of occupation Π_1 and Π_2 of the two dressed states, introduced above, are nothing but the proportions of time spent in dressed states of type 1 and 2 during such a radiative cascade. Every time the dressed atom jumps from a dressed state of type 1 to a dressed state of type 2, or vice versa, the sign of the instantaneous gradient force changes. We thus arrive at the picture of a radiative force oscillating back and forth in a random way between two opposite values. Such an analysis can be made quantitative and provides correct results for the mean value of dipole forces and for the momentum diffusion coefficient associated with their fluctuations [18].

4.2 High intensity Sisyphus effect

We consider now an atom moving with velocity v in an inhomogeneous laser beam, for example an intense laser standing wave, and we try to understand the velocity dependence of the mean force. Velocity damping forces are of course important for laser cooling. Here also, we will consider doublets of dressed states. We will put the emphasis on the correlations which exist, in a standing wave, between the modulations of the dressed-state energies and the modulations of the spontaneous departure rates from these dressed states.

The Rabi frequency associated with a laser standing wave along the

z - axis can be written

$$\Omega_1(z) = \Omega_1 \cos kz \quad (5)$$

Its variation with z is represented in Fig. 7 α . The modulus of $\Omega_1(z)$ is maximum at the antinodes A , at $z = 0, \lambda/2, \lambda, \dots$, where λ is the laser wavelength, and vanishes at the nodes N , at $z = \lambda/4, 3\lambda/4, \dots$. The dashed lines of Fig. 7 β give the energies of the uncoupled states $|a, N+1\rangle$ and $|b, N\rangle$, which are independent of z . We suppose here $\delta > 0$ ($\omega_L > \omega_0$), so that $|a, N+1\rangle$ is above $|b, N\rangle$. The splitting between the two dressed states $|1(N)\rangle$ and $|2(N)\rangle$, represented by the full lines of Fig. 7 β , is $\hbar\Omega(z)$, where, according to (4) and (5)

$$\Omega(z) = [\delta^2 + \Omega_1^2 \cos^2 kz]^{1/2} \quad (6)$$

This splitting is an oscillating function of z . It is maximum at the antinodes A and minimum and equal to $\hbar\delta$ at the nodes N . Each dressed state is also represented in Fig. 7 β with a thickness proportional to its radiative width, i.e. to the departure rate from this state due to spontaneous emission. At the nodes N , $|1(N)\rangle$ reduces to $|a, N+1\rangle$ which is radiatively stable and has no width (we suppose that a is the atomic ground state), whereas $|2(N)\rangle$ reduces to $|b, N\rangle$ which has a width Γ equal to the natural width of the atomic excited state b . When one goes from a node N to an antinode A , the contamination of $|1(N)\rangle$ by $|b, N\rangle$ increases progressively, so that the width of $|1(N)\rangle$ increases from zero to a maximum value at the antinode. Conversely, the admixture of $|b, N\rangle$ in $|2(N)\rangle$ decreases, so that the width of $|2(N)\rangle$ decreases from Γ at the node to a minimum value at the antinode. The radiative widths of the dressed states are therefore spatially modulated as their energies are. The important point here is the correlation which exists between these two modulations and which clearly appears in Fig. 7 β . When one moves along each dressed state, one sees a succession of potential hills, centered at A for $|1(N)\rangle$, and N for $|2(N)\rangle$, and potential valleys, centered at N for $|1(N)\rangle$, and A for $|2(N)\rangle$. In either case, the width of this dressed state is maximum at the tops of the potential hills.

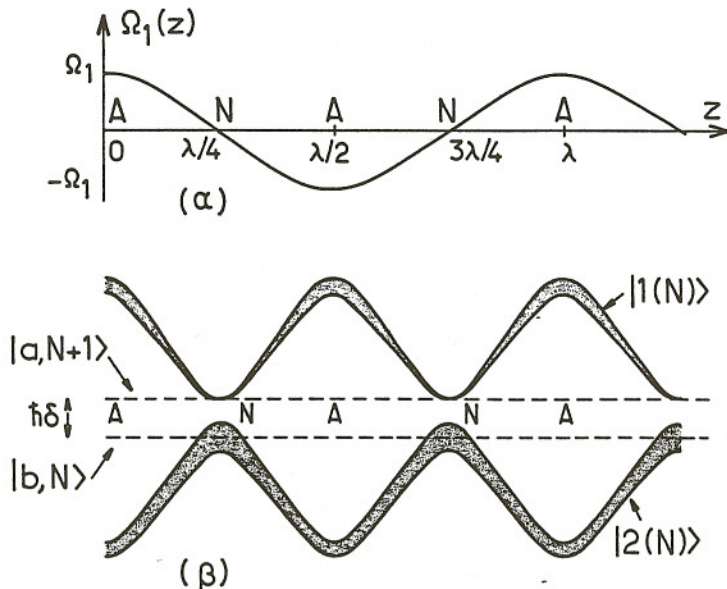


Figure 7: α : Variations of the Rabi frequency $\Omega_1(z)$ along the axis of a standing wave with wavelength λ . The nodes and antinodes are labelled by N and A , respectively.

β : Variations with z of the energies of the uncoupled states $|a, N + 1\rangle$ and $|b, N\rangle$ (dashed lines) and of the dressed states $|1(N)\rangle$ and $|2(N)\rangle$ (full lines). The thickness of the full lines is proportional to the radiative width of the corresponding dressed state. We suppose that $\delta > 0$ ($\omega_L > \omega_0$), so that $|a, N + 1\rangle$ is above $|b, N\rangle$.

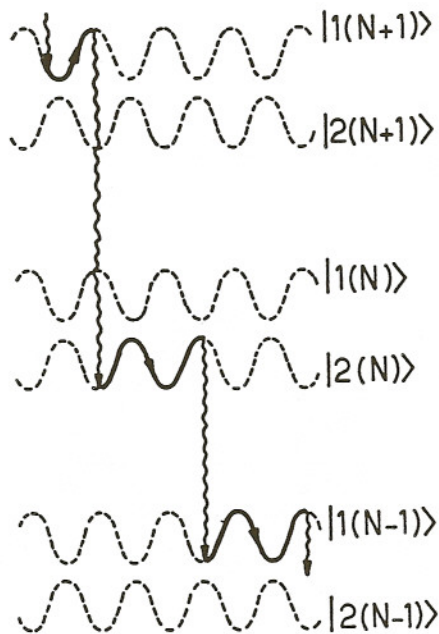


Figure 8: Radiative cascade for an atom moving along a blue detuned ($\omega_L > \omega_0$) intense laser standing wave. The full lines represent the dressed state occupied by the atom between two successive spontaneous transitions (wavy lines). Because of the correlations which exist between the modulations of the energies of the dressed states and the departure rates from the dressed states, the dressed atom is running up potential hills more frequently than down, as did Sisyphus in the Greek mythology.

Suppose now that the atom is moving along the standing wave with a velocity v such that it can travel over a distance of the order of λ in a time Γ^{-1} . The atom can thus remain in a dressed state and go from a node to an antinode, or vice versa, before leaving this dressed state by spontaneous emission. Figure 8 represents a few steps of the radiative cascade of the moving atom. The full lines represent the dressed state occupied by the atom between two successive spontaneous emission processes represented by the wavy lines. According to the previous discussion, the atom has the largest chance to leave a dressed state, be it of type 1 or 2, at the top of a hill. If the atom jumps to the other type of dressed state (from 1 to 2, or from 2 to 1), it arrives in the bottom of a valley from where it must climb to the top of a hill of this new dressed state before leaving it, and so on. We therefore have an atomic realization of the Sisyphus myth, because the atom is running up the potential hills more frequently than down. Such an argument can be made more quantitative [18] and it can explain physically all the features of the velocity dependence of the radiative forces in a high intensity laser standing wave, a problem which has been extensively studied by several authors [19]. Note that we obtain here a velocity damping force for $\omega_L > \omega_0$, whereas the usual Doppler cooling force in a weak standing wave [20] appears for $\omega_L < \omega_0$. Experimental demonstration of the change of sign of the velocity-dependent force at high intensity has been achieved [21]. Evidence has been also obtained for a channeling of atoms in the nodes of a blue detuned standing wave [22].

Note also that similar effects occur for an atom having several Zeeman sublevels in the ground state and moving in a low intensity laser configuration exhibiting a spatially modulated polarization. The light shifts of two ground state sublevels can then be spatially modulated as well as the optical pumping rates from one Zeeman sublevel to the other, the two modulations being correlated in such a way that they give rise to a low intensity Sisyphus effect [23]. Such a laser cooling mechanism turns out to be two orders of magnitude more efficient than the usual Doppler cooling mechanism (see the review

paper [24] and references therein).

Although other physical problems may be analyzed along the same lines, I will stop here, with the hope that I have given an idea of the generality of the basic ingredients of the Autler-Townes effect.

* Laboratoire associé au CNRS et à l'Université Pierre et Marie Curie.

References

- [1] S.H. Autler and C.H. Townes, *Phys. Rev.* **100**, 703 (1955). See also C.H. Townes and A.L. Schawlow, *Microwave Spectroscopy* (Dover, New York, 1975), § 10-9.
- [2] B.R. Mollow, *Phys. Rev.* **A12**, 1919 (1975).
- [3] C. Cohen-Tannoudji and S. Haroche, in *Polarisation, Matière et Rayonnement, Livre jubilaire en l'honneur d'Alfred Kastler*, edited by Société Française de Physique (Presses Universitaires de France, Paris, 1969), p. 191.
- [4] C. Cohen-Tannoudji, J. Dupont-Roc and G. Grynberg, *Atom-Photon Interactions - Basic Processes and Applications*, (Wiley, New-York, 1992), chapter VI.
- [5] C. Cohen-Tannoudji, *C. R. Acad. Sci.* **252**, 394 (1961). See also C. Cohen-Tannoudji and J. Dupont-Roc, *Phys. Rev.* **A5**, 968 (1972).
- [6] J.L. Picqué and J. Pinard, *J. Phys.* **B9**, L77 (1976). J.E. Bjorkholm and P.F. Liao, *Opt. Commun.* **21**, 132 (1977).
- [7] A. Shabert, R. Keil and P.E. Toschek, *Appl. Phys.* **6**, 181 (1975). C. Delsart and J.C. Keller, *J. Phys.* **B9**, 2769 (1976). P. Cahuzac and R. Vetter, *Phys. Rev.* **A14**, 270 (1976).

- [8] T.W. Hänsch and P.E. Toschek, *Z. Phys.* **236**, 213 (1970). B.J. Feldman and M.S. Feld, *Phys. Rev. A* **1**, 1375 (1970). I.M. Beterov and V.P. Chebotayev, *Progress in Quantum Electronics*, Vol. 3, ed. by J.H. Sanders and S. Stenholm (Pergamon Press, 1974). S. Feneuille and M.G. Schweighofer, *J. de Physique* **36**, 781 (1975).
- [9] C. Cohen-Tannoudji, *Metrologia* (Springer Verlag) **13**, 161 (1977).
- [10] C. Cohen-Tannoudji, F. Hoffbeck, S. Reynaud, *Opt. Commun.* **27**, 71 (1978).
- [11] S. Reynaud, M. Himbert, J. Dupont-Roc, H. Stroke, C. Cohen-Tannoudji, *Phys. Rev. Lett.* **42**, 756 (1979).
- [12] B.R. Mollow, *Phys. Rev.* **188**, 1969 (1969).
- [13] F. Schuda, C.R. Stroud and M. Hercher, *J. Phys.* **B7**, L198 (1974). F.Y. Wu, R.E. Grove and S. Ezekiel, *Phys. Rev. Lett.* **35**, 1426 (1975). W. Hartig, W. Rasmussen, R. Schieder and H. Walther, *Z. Phys.* **A278**, 205 (1976).
- [14] C. Cohen-Tannoudji, in "Laser Spectroscopy", p. 324, ed. by S. Haroche, J.C. Pébay-Peyroula, T.W. Hänsch, S.E. Harris (Springer-Verlag, 1975).
- [15] S. Haroche, in *Fundamental Systems in Quantum Optics, Les Houches Summer School Session 53*, ed. by J. Dalibard, J.M. Raimond and J. Zinn-Justin (North-Holland, Amsterdam, 1992). See also the various articles published in *Cavity Q.E.D., Advances in Atomic, Molecular and Optical Physics*, Suppl. 2, ed. by P. Berman (Academic Press, New-York, 1994).
- [16] E.T. Jaynes and F.W. Cummings, *Proc. I.E.E.E.* **51**, 89 (1963).
- [17] Y. Zhu, D.J. Gauthier, S.E. Morin, Q. Wu, H.J. Carmichael and T.W. Mossberg, *Phys. Rev. Lett.* **64**, 2499 (1990). F. Bernardot,

P. Nussenzweig, M. Brune, J.M. Raimond and S. Haroche, *Europhys. Lett.* **17**, 33 (1992). R.J. Thomson, G. Rempe and H.J. Kimble, *Phys. Rev. Lett.* **68**, 1132 (1992).

[18] J. Dalibard, C. Cohen-Tannoudji, *J.O.S.A.* **B2**, 1707 (1985).

[19] See for example A.P. Kazantsev, *Sov. Phys. J.E.T.P.* **39**, 784 (1974).

[20] T.W. Hänsch and A.L. Schawlow, *Opt. Commun.* **13**, 68 (1975).

[21] A. Aspect, J. Dalibard, A. Heidmann, C. Salomon, C. Cohen-Tannoudji, *Phys. Rev. Lett.* **57**, 1688 (1986).

[22] C. Salomon, J. Dalibard, A. Aspect, H. Metcalf, C. Cohen-Tannoudji, *Phys. Rev. Lett.* **59**, 1659 (1987).

[23] J. Dalibard, C. Cohen-Tannoudji, *J.O.S.A.* **B6**, 2023 (1989).

[24] C. Cohen-Tannoudji, W.D. Phillips, *Physics Today* **43**, 33 (1990).